

Vortex flow eddy street behind a circular cylinder superimposed to simultaneous rotation and cross-section variation in uniform flow

OUALLI * H., HANCHI* S., BOUABDALLAH ** A., ASKOVIC*** R.

* *Laboratory of Fluid Mechanics, EMP, Bordj el Bahri, Alger, Algérie*

** *LTSE, Université des Sciences et de la Technologie (USTHB), Alger, ALGÉRIE.*

*** *LME, UVHC, 59313 Valenciennes Cedex 9, France.*

Summary:

In this study we describe the wake response associated with an experimentally simulated flow around a circular cylinder that is either stationary, in steady rotation, in simple harmonic cross-section variation or executing a combination of these dynamics. Results are examined for a Reynolds number range extending from $Re=1000$ to $Re=22000$. The amplitude of the pulsatile motion is fixed equal to 5% of the cylinder diameter. A large domain of the forcing Strouhal number, up to the natural shedding frequency, is considered. The results are interpreted using an analysis of vorticity generation and convection from the base region of the cylinder in the Von Kármán eddy street. The study is focused on a description of the cylinder wake behaviour and specifically on the Von Karman eddy street response to the applied controlling strategy. It is suggested that a non linear combination of Magnus and cross-section variation effects can lead to interesting results on the optimization of the lift to drag ratio.

Introduction:

The description of the wake behind bluff bodies in a vortical flow is of fundamental importance in many scientific fields. The canonical case of the circular cylinder has been the subject of an active research in the last five decades, concerning experimentations as well as numerical investigations. The interest in body rotation is essentially motivated by the possibility of modifying the wake generated downstream and the forces created on the body. Such studies shed light on mechanisms that reduce drag forces, which is a central aspect in aero and hydrodynamics.

Fluid flows over circular cylinders arise in many engineering situations, such as in transmission lines, heat exchangers, marine cables, flexible risers in petroleum production and mooring lines and several other industrial applications, Blevins 1990; Ramberg et al. 1976... It is important to understand the flow dynamics of the cylinder wake and motion of the structures generated by the presence of the body in the flow.

The cylinder motion considered in the present paper is a uniform rectilinear motion with steady rotation and sinusoidal variation of the cross-section. Four governing non-dimensional parameters are defined, namely, the Reynolds number $Re = U_{\infty} D / \nu$, where D is the diameter of the cylinder, U_{∞} is the freestream velocity and ν the kinematic viscosity, the shedding Strouhal number $St = f D / U_{\infty}$, where f is the natural shedding frequency, the forcing Strouhal number $St_f = f' D / U_{\infty}$, where f' is the controlling frequency applied to the cylinder through the cross-section variation, and the steady rotating speed $\alpha = \Omega R / U_{\infty}$, where Ω is the cylinder rotating rate and R is the cylinder radius.

The present experimental investigation of the Von Karman eddy street behind a circular cylinder superimposed simultaneously to steady rotation and diameter variation is an initial step towards understanding the intricate flow phenomena resulting from such combined active control techniques (rotation and radial vibration).

Experimental set-up

These experiments are carried out in an open circuit channel facility EV 280 type. It consists of a low speed air turbine (0.3 - 3 m/s) with a large plexiglas tunnel, approximately 1.5 m long, 0.35m height and 0.45 wide with optical access from all sides. The background streamwise disturbance level is less than 1% of the free stream velocity.

The cylinder made of PVC (Polyvinyl Chlorine) wall, fig. 1 (a) and (b) is mounted horizontally traversing the test section with the ends linked to two external motors so as to deliver rotating motion of the cylinder and cylinder wall vibration as well. The inside of the test cylinder, as shown by fig. 1 (b), consists of the cylinder shaft entrained in rotation motion (by means of the external motor), rotating cams appropriately transform the rotating motion into diameter variation movement of the test cylinder wall according to the following law:

$$R = R_0 (1 + |As \sin (2\pi \times f' \times t)|) \quad (1)$$

where R is the variable cylinder radius, R_0 is the initial cylinder radius, As is the maximum deforming amplitude set equal to 5% of the cylinder diameter, f' is the cylinder forcing frequency in Hertz and t is time in seconds. Considering the cylinder dimensions, the above relation becomes:

$$R = 0.04 (1 + |0.005 \sin (2\pi \times f' \times t)|) \quad (2)$$

The internal deforming system of the cylinder and the test section dimensions imposed an aspect ratio of 5.62. The flow visualizations are performed by releasing a horizontal smoke sheet in front of the cylinder created by injecting smoke through a tubing of a smoke generator enabling a steady leakage of smoke through the oncoming flow.

The collection of flow visualization images is taken with a digital video camera (DVCAM SONY DSPVCL-718 BX) in a rate of 24 images per second. The rotating movement is generated by an electrical motor developing a rotation speed N varying from 0 to 300 rpm.

The arrangement of the circular cylinder in the test section and the apparatus of achieving forced radial oscillations combined to a steady rotation are illustrated in fig. 1. The cylinder axis is clamped to an electrical motor (Malabo CC, RL1 type, EXC Hunt) and constrained to move in a rotating motion to generate the vibrating motion of the cylinder cross section via the integrated mechanism inside the cylinder. The cylinder wall is thus forced to oscillate back and forth in a sinusoidal profile by means of “cams” linkage. The rotating cams mechanism converts the rotary motion of the drive shaft into sinusoidal motion of the cylinder wall. The entire mechanism is mounted inside a cylindrical PVC housing so that no protruding elements and thus perturbations are introduced in the test section.

The cylinder wall is entrained in a steady rotation by a second electrical motor (identical to the first). The motor rotating speed can be set in the range 0-300 rpm. With this system, the corresponding forcing Strouhal number, $St_f = f' D / U_\infty$, is between 0 and 15.

The non dimensional steady rotating speed considered in this study, $\alpha = \Omega R / U_\infty$, extends on the wide range of 0 to 11.78.

The results are presented for $Re=3000$, flow visualizations are carried out to study the behavior of the cylinder near wake in response to combined steady rotation and radial vibration control techniques.

The present investigation of the near wake of a circular cylinder superimposed simultaneously to steady rotation and diameter variation is an initial step towards understanding the intricate flow phenomena generated when such active control techniques (rotation and radial vibration) are coupled on the forced cylinder.

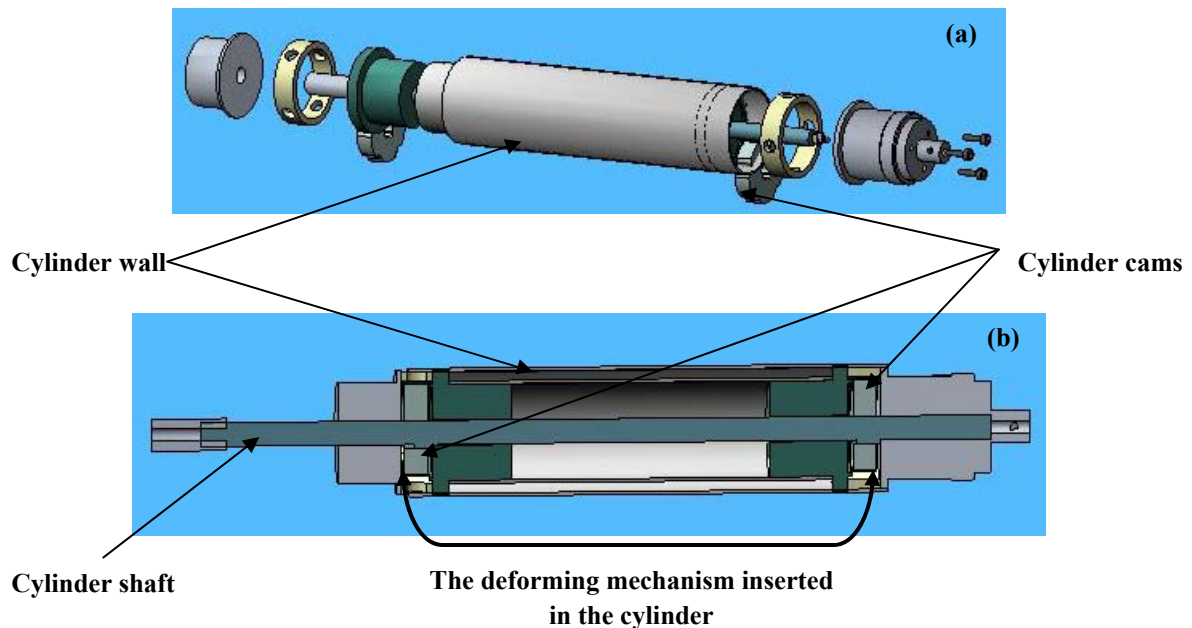


Fig. 1: Experimental test and cylinder deforming mechanism

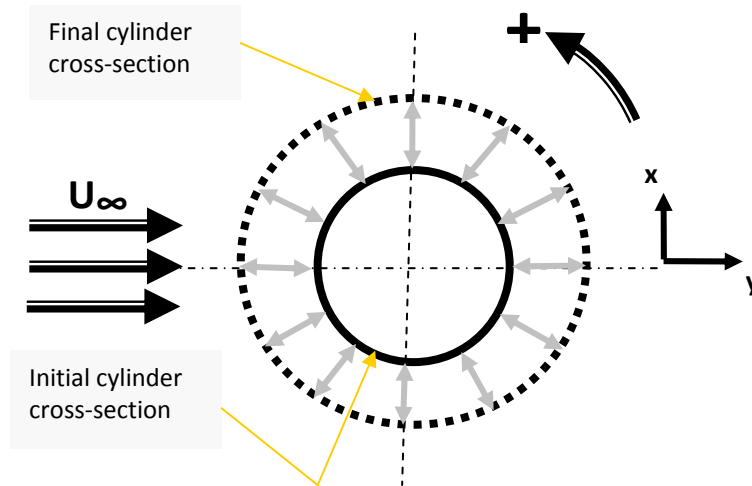


Fig.2: Schematic diagram of the actuating technique

Results and discussion:

A first understanding of the visualization results is deduced from the captured digital images. Separation of the successive video frames into digital images enables compilation of time sequences showing evolution of the vortices interactions, the vortex shedding mode and the von Kármán eddy street. The original visualization results quality is improved using suited software. Dye streaks contours are detected and highlighted to interpret the results more clearly. These tracings scale-accurate representations of the near wake region, showing the surrounding shear layers and the primary vortices in the eddy street behind the cylinder.

The vortex shedding Strouhal number, St , for the non-controlled cylinder at a freestream velocity of $U_\infty=3 \text{ m/s}$ is determined to be 0.21. This value is in excellent agreement with the universal $St-Re$ relation. The considered Reynolds number, $Re=3000$, coincides with the subcritical flow regime for which the Strouhal number fluctuates in the range of 0.18-0.22, Roshko (1954) and Zdravkovich (1997). The visualized near wake region for this nominal case at a time where the vortex formation is fully developed is shown in figure 3.

The shear layers and the vortex roll-up surrounding the formation region are clearly illustrated on this figure. The shear layers rolling-up and the von Kármán vortices are formed following a laminar fashion, without undulations of the shear layers, indicating the absence of Kelvin-Helmholtz instability vortices on the shear layers. Tokumaru (1991) carried out experiments for an active control of a circular cylinder using a rotative-oscillating technique for $Re=15000$, corresponding to the same flow regime. A similar flow pattern of Tokumaru (1991) nominal case can be seen in fig 4.

The fig. 3, depicts the nominal case considered as a reference measurement for comparison with visualization results obtained for an actuated cylinder, superimposed to both radial vibration and steady rotation.

When the cylinder is set into control the flow developed various modifications and phenomena in response to the applied actuating perturbations. We limit this study to the observations illustrating the important modifications on the von Kármán eddy street specifically.

When examining the sequences of the acquired pictures, several shedding modes are identified throughout these flow visualisations. Particularly, we identified the four modes presented by Tokumaru (1991) for a cylinder submitted to rotative oscillations and termed *dual shedding mode*, *global locking mode*, *local locking mode* and *the shear layer mode* but as partial modes in our study, Oualli et al (2004, 2007).

According to Tokumaru (1991), these shedding modes are accompanied by a drastic reduction of the drag coefficient up to 80% of the non controlled case. Furthermore, an interesting feature of this flow is the progressive and ordered way each mode evolves at the selected values of the frequency and steady rotation of the cylinder.

In the fig. 3, the wake flow is parallel to the midspan plan (straight and without beating motion) the shear layers developed instabilities as undulations and kinks without evolving to roll-ups vortices as it can be expected.

Williamson and Roshko (1988) and Païdoussis (2001) observed the occurrence of such double roll-ups appearing in the formation region induced by the cylinder acceleration.

In our experiments, the wake beating movement is not limited to the formation region but extends to farther wake behind the cylinder. This undulation phenomenon is thought to be caused by the cylinder wall acceleration during the radius increasing and decreasing motion.

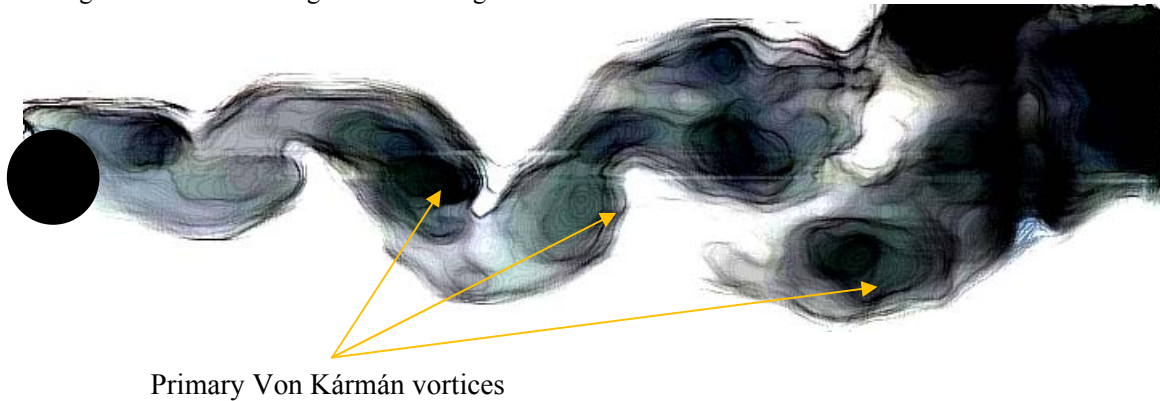


Fig. 3: A von Karman eddy street in the (2S) mode behind a non actuated cylinder/ (natural case) at $Re=3000$ - Present results

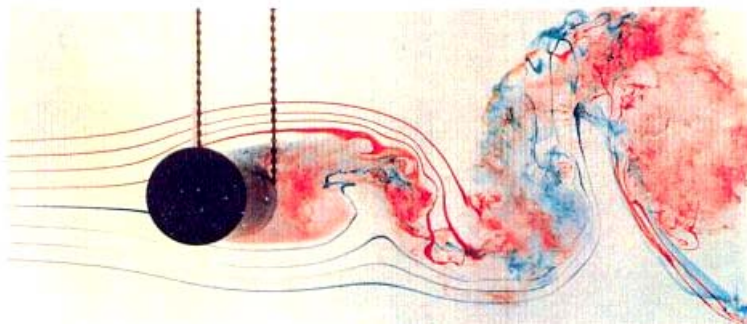


Fig. 4: A von Karman eddy street behind a non actuated cylinder at $Re=15000$ (2S) shedding mode /Dimotakis Ph.D. thesis (1991)

In fact, the Kelvin-Helmholtz instability settling in the flow shear layers is strongly enhanced. This tendency is immediately reversed by the steady rotation effect of the cylinder which attenuates the developing instability preventing, thus, roll-ups vortices formation. The applied steady rotation, when it is clockwise executed, seems to strongly contribute to the cylinder wake straightening.

The rotation movement is expected to deeply alter the wake flow pattern and eddy street behaviour. The basic physical rationale of the rotating effect concerns the accelerated flow of the upper side of the cylinder leading to the separation delay or suppression. The flow over the lower side is, however, decelerated and subject to premature separation. Hence, the pressure on the accelerated side becomes smaller than that of the decelerated side, resulting in an enhanced mean lift force (this effect is known as “Magnus effect”), Homescu et al. (2001).

The wake configuration is clearly seen to be of (2P) type in fig. 5. Two vortex pairs are shed per cycle of a radial cylinder oscillation and the vortex pairs rapidly diverge away from the wake axis. The (2S) type wake pattern shown in fig. 3, where two vortices are shed from the circular cylinder per shedding cycle is markedly different from the (2P) mode shown in fig. 5. In the former (2S) mode, the vortices remain close to the wake axis as they convect downstream. The latter wake pattern (2P mode) is seen as indicating synchronisation with respect to cylinder motion as reported by Païdoussis (2001) and Williamson and Roshko (1988).

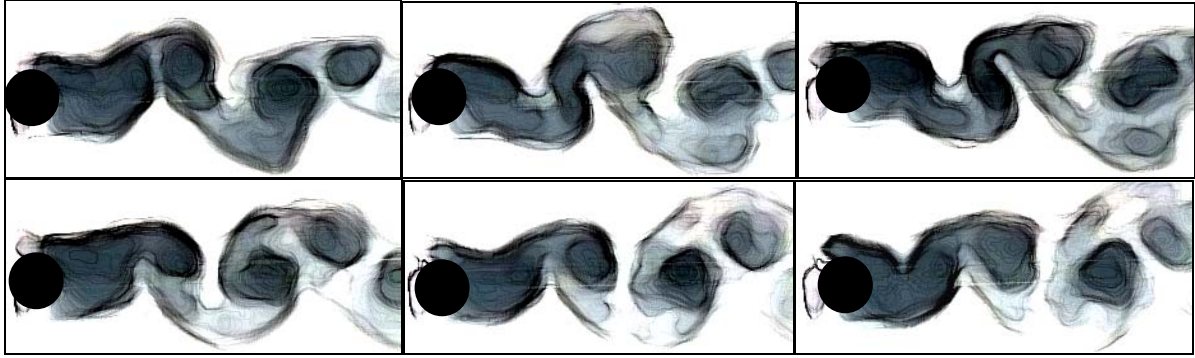


Fig.5: (2P) shedding mode for $\alpha = 0.175$ and $St_f = 0.47$

The coherent synchronized wake patterns observed for the excitation regime frequencies within the synchronized regime (composed of the (2P) regime) is not preserved indefinitely over the oscillation cycles. Flow visualization results of the near wake and formation regions illustrating its evolution are given in fig. 6 corresponding to oscillation frequency $St_f=0.47$.

Comparing the images of this figure shows that the regular (2P) mode shifts progressively to a new (2P) mode characterized by a horizontally beating wake and a variable wave number of the Von Kármán eddy street forming behind the cylinder with a rate of roughly 35% as estimated from the visualisations. The observed periodic variation of the instability wavenumber is seen in the current experiments to be accompanied by a substantial increasing and decreasing of the vortex formation length, as shown in the fig. 6.

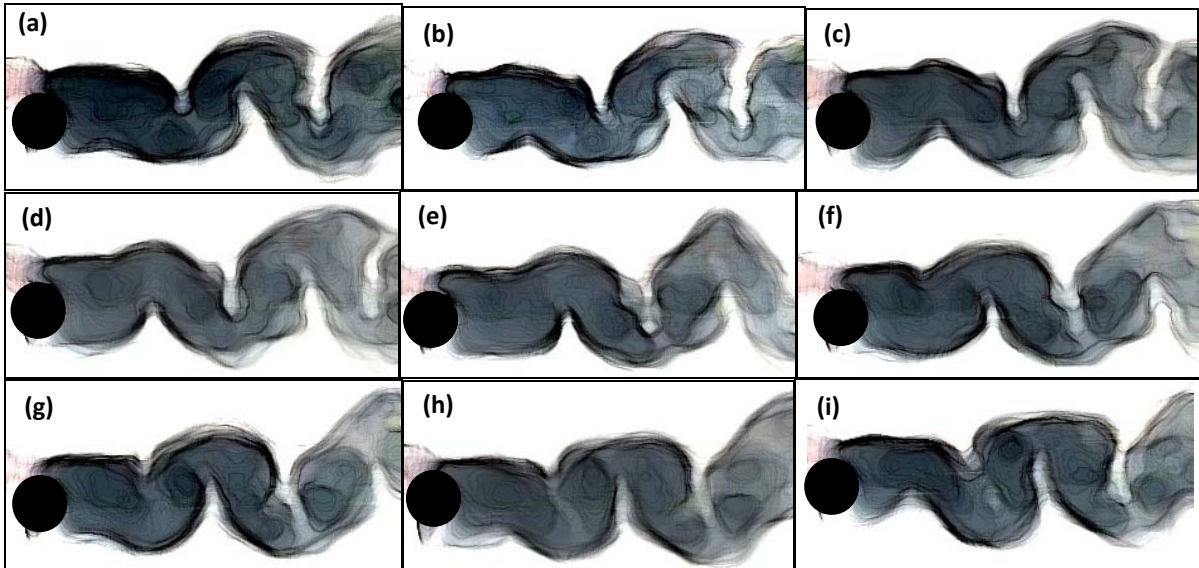


Fig.6: (2P) shedding mode for $\alpha = 0.175$ and $St_f = 0.47$ / wavelength variation at $Re=3000$

An attempt to quantify vortex formation lengths for a cylinder vibrating frequencies in the range, $0.37 \leq St_f \leq 15$ with the steady rotation, $\Omega_1 = 23$ rpm, is maintained constant.

While the vortex formation length is rather well defined for flows past a stationary cylinder, difficulties arise when the cylinder is forced to vibrate radially and rotate steadily around its axis, for the following reasons:

(i) The shear layer shed from the cylinder are subject to alternating repulsion and attraction movement induced by the cross-section increasing and decreasing respectively. Time histories of the instantaneous velocity experimentally sensed using hot-wire probes at a distance up to $10D$ downstream of the vibrating cylinder clearly illustrate this effect when the vibrating frequency is increased as depicted in the fig. 7. The peaks appearing in the velocity time evolution are explained by the radial outward jet flow induced by the cylinder cross-section increasing. The number of peaks is directly dependent on the applied frequency of the oscillating motion.

(ii) There are several vortex processes contributing to vortex formation:

- Those applicable to natural vortex formation from a stationary cylinder (Gerrard (1966), Zdravkovich (1997), Coutenceau et al. (1985)),
- Shear layers undulations in the shear layers (in the form of roll-ups successions) mainly induced by the radial acceleration of the cylinder wall with the cross-section variation.
- The interacting mechanism of the vortices and the shear layers which is highly intricate.

(iii) Coutenceau and Ménard (1985) reported that the more important effects of the steady rotation are:

- Inducing of a continuous fluid layer that rotates with the cylinder in such a way that the stagnation and separation points around the cylinder are shifted from the wall within the stream. The thickness of this layer is found to increase with the rotating rate but decreases with Reynolds number increasing.
- Destroying of the vorticity symmetry generated from the cylinder because of the difference between the relative fluid-to-wall velocity on each side of the cylinder (one side moving in the freestream direction and the other moving oppositely). So, eddies with different size and strength are created.
- Eddies detachment is accelerated and the vorticity evacuating process within the stream is thus enhanced.

Representative vortex formation lengths L_f are estimated as suggested by Païdoussis (2001), L_f is the streamwise distance from the axis of the cylinder to the core of fully formed vortex, at several vibrating frequencies with a fixed cylinder rotating speed were determined in the first case and for a fixed vibrating frequency and various rotating speeds in the second case.

This formation length is evaluated from the visualization images of the formation region in which a fully formed vortex was clearly seen when the shear layers were quasily straight. The results are represented in the figure 7 (a and b). In the first case, the vortex formation length is evaluated for the fixed rotating non-dimensional rate $\alpha = \Omega D/2U_\infty$ equal to 1.78.

As the forcing Strouhal number, St_f , is augmented, the formation length increases with a jump of 73% before decreasing in a rather sharp way to reach a minimum value of $L_f/D = 1.9-2$ at $St_f = 2.96$. As the forcing Strouhal number is increased above 3.64 the formation length seems stabilizing around a constant value of $L_f/D=3$.

In the second case, the forcing Strouhal number is put equal to 6.60 while the rotating rate α is varied in the range 8.74 to 11.5.

As the rotating rate is increased the vortex formation length becomes gradually greater until it reaches a maximum of about 54% higher than the formation length in the natural case (stationary cylinder) at $\alpha = 8.90-9.44$. Then, the formation length decreases abruptly as the rotating rate is increased from 9.52 to 11.15. This tendency seems to be persistent for the higher values of α .

It comes out from the above results that an optimization value of the lift to drag coefficients ratio, $(C_L/C_D)_{opt}$, can be obtained for an optimal vortex formation length reduced by a rightly determined value of the rotation rate α_{opt} and maintained around this value by fixing the right value of the forcing Strouhal number $St_{f,opt}$.

Jeon et al. (2004) established that the lift is directly linked to the vortex circulation in the formation region via the relation:

$$lift \approx -\frac{d}{dt}(\rho x \Gamma) = -\rho(\Gamma \dot{x} + x \dot{\Gamma})$$

Where Γ refers to the circulation of that vortex and x its position downstream from the cylinder.

The drag coefficient is given by Sheils and Leonard (2000) considering the drag expressed from the vorticity function perspective:

$$Drag = -\rho \frac{d}{dt} \left(\iint_A y \omega dA \right)$$

Where y is the cylinder transverse direction and the area A represents the entire flow field in which the vortex structures shed from the body contain significant components.

Consequently, a convenient actuation of the shed vortices can result in an optimal ratio $(C_L/C_D)_{opt}$.

According to Jeon et al. (2004), the vortex formation mode can be seen as evolving in three stages: initial vortex growth, saturation, growth of a trailing shear-layer-like structure. At early times, the separating boundary layer rolls up into a vortex. However, this process reaches saturation at some point, as the vortex is of finite size. Afterwards, any additional vorticity in the separated boundary layer ends up in a shear-layer-like structure connecting the vortex back to the generator.

The vortex then undergoes “pinch-off” and separates from the boundary layer that provided its circulation.

To explain wake changes and inter-modal switching, Jeon et al. (2004) offered an alternative explanation to the classical view mapped on the changing flow conditions based on the concept of vortex formation time (and length).

What role does the transition to the (2P) state have to do with the vortex formation process?

In an attempt to answer this question, Jeon et al. (2004) reported that the (2P) mode is where two pairs of vortices are shed as dipole pairs per side per cycle. If the cylinder were to accelerate in forward during formation process, there would less time for the vortex to form before it sheds. Since the (2P) mode appears along the formation region side, it is believed that there is a connection between long formation and the (2P) mode appearance. Jeon et al. (2004) made the supposition that the second vortex in the pair forms from a secondary roll up of the connecting shear layer in the sense of Kelvin-Helmholtz instabilities and hence is just a by-product of long formation time.

This portrayal of the (2P) appearance seems to be appropriate for a cylinder superimposed to streamwise acceleration as considered by Jeon et al. (2004).

In the present study, the cylinder is subjected to neither transverse nor streamwise acceleration and the (2P) mode is albeit clearly identified as the persistent mode. Furthermore, the presence of the (2P) mode is not systematically conditioned by a formation length higher to the natural one ($L_f/D \approx 4$). Fig. 6 shows a cylinder wake evolving in the (2P) mode with a formation length $L_f/D \approx 1.5$. This indicates that the (2P) mode is likely of multiple genesis mechanisms.

In our case the question still remains, but the near wake structures phenomenology (migration and coalescence induced by rotation as described by Coutenceau and Ménéard (1985) interacting with the bulge phenomenon, prior to phenomena α and β based upon the secondary and tertiary vortices) is expected to lead to such arrangement of the Kármán eddy street structures. The occurrence of the (2P) mode can be elucidated by analysing the relation between these in response to the forcing dynamics (radial vibration and steady rotation).

The (2P) mode is identified to be the most dominant configuration of the wake as the cylinder is submitted to such a control. Various flow features and properties are recognized to characterize this flow mode.

Sungho et al (2002) noted that the merging phenomenon is a typical aspect of the controlled flows. The authors reported that the forcing frequency determines the numbers of vortices involved in the vortex merging phenomena (1, 2, 3, and 4) and the forcing amplitude decides the order of the vortex merging mode during one modulation period.

This coalescence phenomenon of the subscale primary vortices combined to both the interaction with the secondary vortices in the vicinity of the obstacle and the superimposed frequency constitute the basic explanation of the drag modulation phenomenon.

Cerretelli and Williamson (2003) stimulated by experimental observations of vortex merging computed a new family of vorticity structures which pass from the limiting case of point vortices through the case of two-equal co-rotating uniform vortices to the regime where the vortices touch in the form of a “dumb-bell”.

The merging phenomenon is actually present in the (2P) mode but in several processes. The vortices coalescence in the way portrayed by Cerretelli and Williamson (2003) is frequently met in the near wake as the cylinder rotating rate and vibrating frequency are increased but for counter-rotating vortices case. Two counter-rotating vortices, respectively ordered in the von Kármán eddy street, fully developed and shed from the vortices formation region are progressively slowed down in the near wake. The vortices centres getting closer from each other, tangentially touch and the boundary between the merging structures increasingly vanishes to completely disappears with the nascent resulting structure. At the end of this merging mode a new structure of larger scale appears in the cylinder wake and convects downstream in the cylinder wake. The first main characteristic of this merging mode consists in the fact that when merging, the involved structures decelerate substantially till the resulting structure is completely formed and the vortices coalescence mode is fully achieved.

The second characteristic concerns the resulting structure which swiftly dislocates when travelling in the wake leading to its rapid decay by diffusion while the non-merged structures persist much farther in the cylinder. The second merging mode revealed by the flow visualisations, seems to be original in literature since created by the present control situation. Three shed structures coalesce in a mechanism remarkably similar to the blood leucocytes operating a “phagocytise” in bacteria ingestion and destruction.

Two successive vortices (evolving in the cylinder wake in the immediate vicinity of the vortices formation region) merge first, evolve to an open “crown shape” before surrounding the neighbouring third structure in the wake. The latter is partially broken and the encircled part is engulfed in a swirling motion leading to a new vortical structure occurrence as illustrated in the fig. 9.

Conclusion

Quantitative and qualitative flow characteristics of the wake behind a circular cylinder submitted to a sinusoidal cross-section variation as a first step of this study and a steady rotation combined to cross-section variation as a second step are experimentally investigated.

In the first case of the merely vibrating cylinder, hot wire results showed that the influence of the applied controlling technique extends up to ten diameters downstream in the cylinder wake. This influence manifests in peaks appearance in the streamwise velocity time history induced by the cylinder cross-section increasing phase.

The decreasing phase behaviour seems to be more intricate with a particularly strong influence on the primary and secondary structures interaction in the cylinder vicinity resulting in a reduced strength and scale of the von Kármán vortices.

In the second case of the combined steady rotation and cross-section variation several features and phenomena are observed. A remarkable similarity with the evolution reported in several studies devoted to rotative oscillation is illustrated.

When the main controlling parameters, α and St_f are varied, the (2P) mode seems to prevail throughout the spanned ranges of the steady rotation rate and forcing Strouhal number.

To answer the central question related to the optimization of lift to drag coefficients ratio, it is accomplished that the obtained results favourably encourage further quantitative exploration in order to exactly explain the mechanism of the observed physical features.

References

- [01] **Roshko, A. (1954)** “ On the development of turbulent wakes from vortex streets”. Ph. D thesis, California Institute of Technology, Pasadena, California
- [02] **Zdravkovich, M. M. (1997)** “Flow around circular cylinders”. Vol. 1: Fundamentals. Oxford University Press, Oxford, England.
- [03] **Tokumar P. T., (1991)** “Active control of the flow past a cylinder executing rotary motions”. Ph.D thesis, California Institute of Technology Pasadena, California.
- [04] **Oualli H., Hanchi S, Bouabdallah A., Askoviç R. (2004)** “Experimental investigation of the flow around a radially vibrating circular cylinder”, *Experiments in fluids* 37, 789-801.
- [05] **Oualli H., Hanchi S., Bouabdallah A., Askoviç R., Gad-El-Hak M. (2005)** “Drag reduction in a radially pulsating cylinder at moderate Reynolds number”, *Bulletin of the American Physical Society*, vol. 50, N°9, 56.
- [06] **Williamson, C. H. K. and Roshko, A. (1988)** “Vortex formation in the wake of an oscillating cylinder”. *Journal of Fluids and Structures* 2, 355-381.
- [07] **Krishnamoorthy, S., Price, S. J. and Paidoussis, P. (2001)** “Cross-flow past an oscillating circular cylinder: Synchronization phenomena in the near wake”. *Journal of Fluids and Structures* 15, 955-980.
- [08] **Homescu, C., Navon, I. M. and Li, Z. (2002)** “Suppression of vortex shedding for flow around a circular cylinder using optimal control”. *Int. J. Numer. Meth. Fluids*, **38**, 43-69.
- [09] **Gerrard, J. H., (1966)** “The Mechanics of the Formation Region of Vortex Behind Bluff Bodies”. *J. of fluid Mech.* 25, 401-413.
- [10] **Coutanceau, M. and Ménard, C. (1985)** “Influence of rotation on the near-wake development behind an impulsively started circular cylinder”. *Journal of Fluid Mechanics* 158, 399-446.
- [11] **Jeon, D. and Ghrib, M. (2004)** “on the relationship between the vortex formation process and cylinder wake vortex patterns”. *J. Fluid Mech.* **519**, 161-181.
- [12] **Shiels D., Leonard A. (2001)** “Investigation of a drag reduction on a circular cylinder in rotary oscillation”. *J. Fluid Mech.* 431, 297-322.
- [13] **Seung-Jin B., Sang, B. L. and Hyung J. S. (2001)** “Response of a circular cylinder wake to superharmonic excitation”. *J. Fluid Mech.* (2001), vol. 442, pp. 67-88.
- [14] **Cerretelli, C. and Williamson, C.H.K (2003)** “A new family of uniform vortices related to vortex configurations before merging”. *Journal of fluid Mechanics*, 493, 219-229.

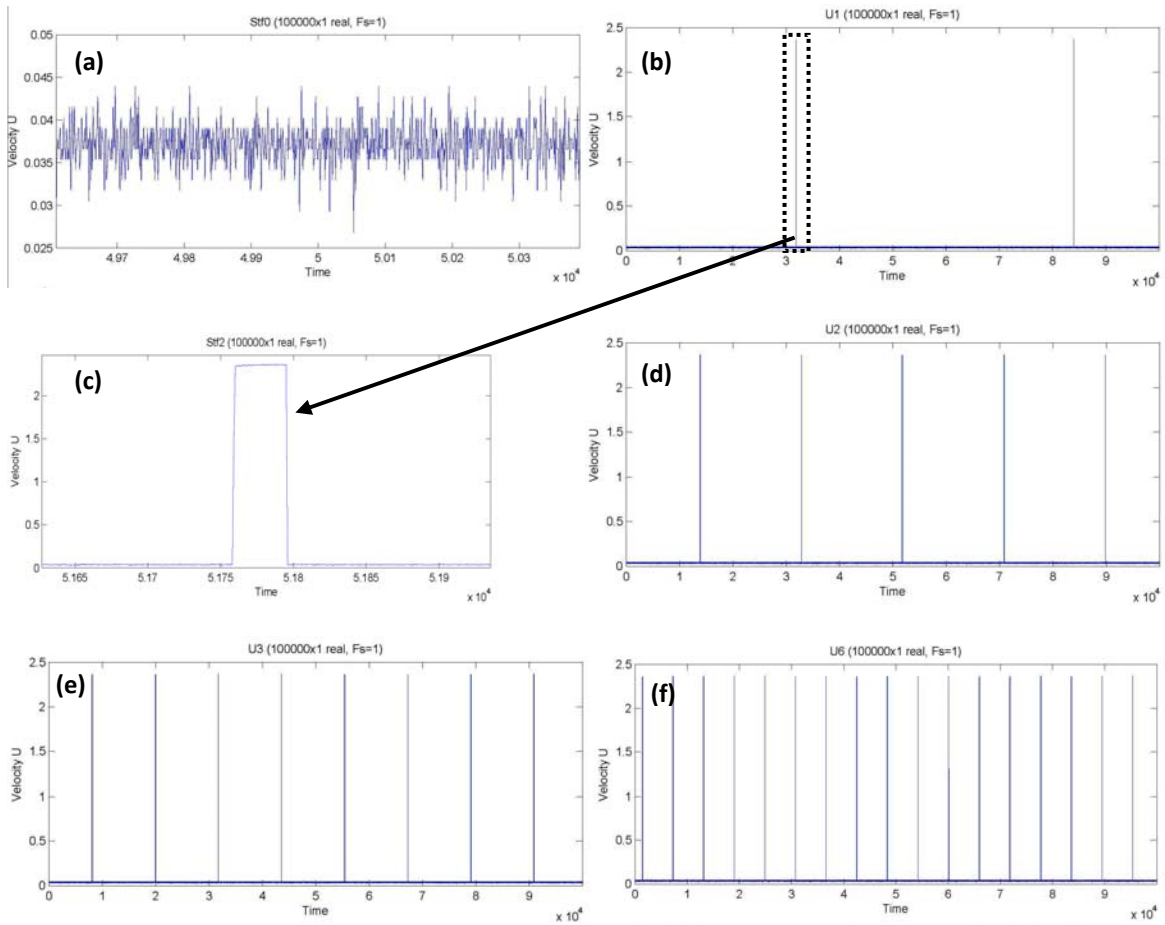


Fig.7: Time traces of the instantaneous velocity sensed using hot wire probe at a distance of 10D downstream of the cylinder, (a) non-controlled cylinder, (b)-(d)-(e) and (f) deforming cylinder with an increasing frequency, (c) a zoomed peak

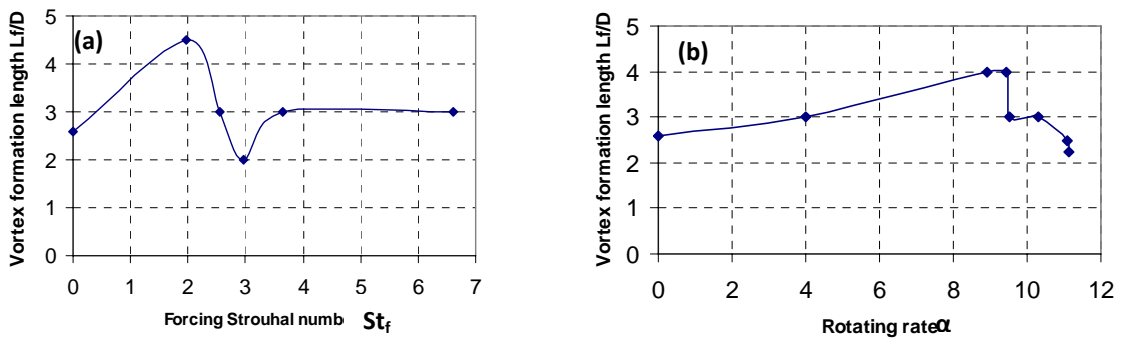


Fig.8: Evolution of the vortex formation length “ L_f/D ” at $Re = 3000$

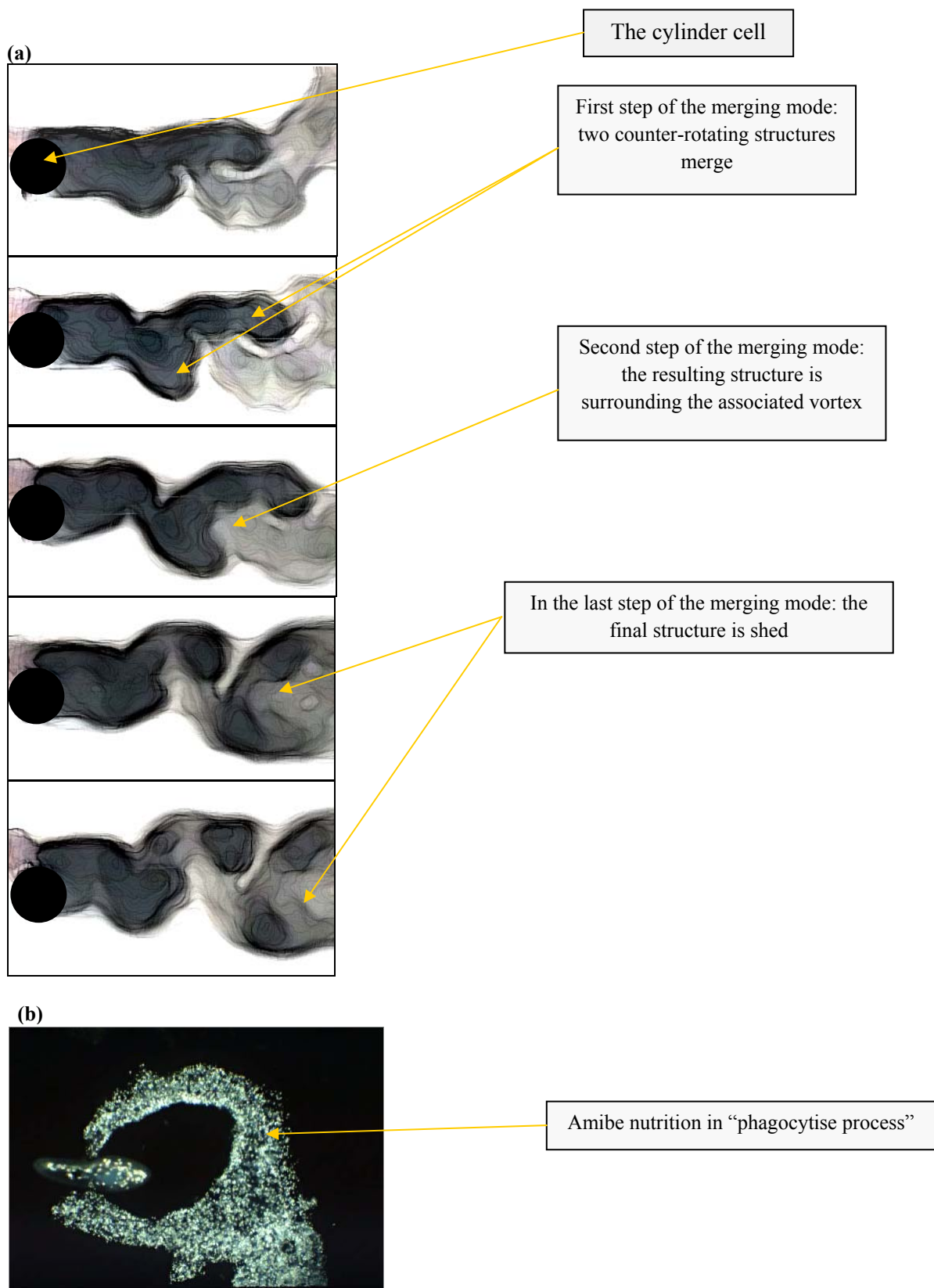


Fig. 9: Merging phenomenon at $Re = 3000$; (a) Three vortices coalescence as a leucocytes or compared to Amibe nutrition "Phagocytise process"

